

Identifying Fracture Growth Patterns Using Microseismicity

T.I. Urbancic, S.C. Maxwell, C. Demerling - ESG and R. Zinno - Schlumberger

CSEG Geophysics 2002

As shown in numerous examples (e.g., see Maxwell et al., these proceedings), passive seismic monitoring offers the opportunity to image the dimensions of hydraulic fractures. Images are typically obtained by evaluating the distribution of event locations in both space and time. One of the benefits of passive seismic monitoring, is the additional characteristic information that is inherently available in the recorded signals. As in earthquake seismology, these signals provide insight into the nature of the forces acting at the source and the seismic event generation process. Specifically, information can be obtained on the strength of the event (seismic moment, moment magnitude), effective seismic energy release (P- and S-wave energy release), the stress release (static stress drop and apparent stress release), mechanism of failure (S-wave to P-wave seismic energy ratio, focal mechanisms), and slip dimensions (source radius, fault length).

Not all of these parameters, however, are robustly calculated due to limitations in recording (most stimulations are monitored from a single well, limiting the spatial coverage of the event source volume) and the apparent assumed models of failure for these events. Some parameters do provide relatively independent and robust estimates of source attributes. One of these is the apparent stress drop, which effectively represents the average stress released on fractures as a result of changes in stress conditions at the source (i.e., shear stress versus normal stress). For example, treatments where fluid interacts with pre-existing fractures, an effective decrease in resisting stress without an increase in driving stress can generate microseismic events. Characteristically, these events would likely result in low apparent stress drop values. Conversely, tight non-opened fractures would likely fail under higher driving stress conditions as resistive stresses would be higher, resulting in larger values of apparent stress (Urbancic and Zinno, 1998).

By looking at the spatial and temporal distribution in apparent stress, we can effectively identify differences in the stress state leading to the development of the hydraulic fracture. To this end, we have analyzed a series of treatments carried out in the Cotton Valley, East Texas. Monitoring was carried out from a single well, with a 12 level retrievable array of triaxial geophones located above the reservoir within close proximity to the treatment well (see Figure 1). Prior to the stimulation, the array of geophones were clamped in place and perforation shots in the treatment well were recorded and used to determine the orientation of the individual geophone sondes. Signals were continuously monitored and a complex trigger logic was employed to discern events from background noise in real-time (Maxwell et al., 2000). The events were automatically located and their source parameters (corrected for attenuation) determined. Visual images of the stimulation, such as those shown in Figure 1, were obtained in real-time and combined with engineering data (oblong shape wireframe represents the 2-D fracture mechanics model output and red / blue time based chart, in this case, represents the surface pressure and proppant concentration, respectively).

In Figure 1, the distribution of apparent stress drop values for microseismic events as recorded at four sequential stages of a stimulation are shown. A number of clearly defined trends can be easily identified. In general, the leading edges of the fracture development tend to have higher apparent stress release values (orange – red) than those behind the fracture front, which generally exhibit low stress drop values (green). We suggest that these observations may represent changes in the growth characteristics of the hydraulic fracture, with shear driven failures at the extremities of the fracture and failures due to unloading (decrease in normal stress) occurring behind the fracture front; it is this later response that may be further representative of volumetric behavior of the propped zone.

Additionally, the observations clearly show that the introduction of proppant (Figure 1b), resulted in a significant growth of the fracture towards the monitoring well (right). Interestingly, the final distribution in microseismicity (Figure 1d) is quite asymmetric, with very little growth occurring to the left of the treatment well. As well, the limitations of the fracture mechanics model employed are quite evident, as it can only predict symmetric responses to stimulations.

To consider if the asymmetric response was influenced by the recording set-up (use of one monitoring well), a comparison was made between all the stimulations monitored in the same field (Figure 2). In each case, the strike of the main fracture was calculated by linear regression, and the angle between its normal and the monitoring well relative to the treatment was determined. As shown in Figure 2, the angle to the fracture varies by over 50 degrees. The degree of symmetry generally falls into three categories, 1 to 1, 2 to 1, >2 to 1 (in the last case, the higher asymmetry may be related to data quality issues). Upon closer examination of the data, the variations can be related to treatments in different lithologic layers, suggesting that the recording set-up did not influence the outcome and that the observed distributions in microseismic values are representative of the fracture growth behavior occurring in the field.

References

- Maxwell, S.C., Urbancic, T.I., Falls, S.D., and Zinno, R., Real-time Microseismic Mapping of Hydraulic Fractures in Carthage, Texas, Ann. Mtg., SEG, 2000.
- Maxwell, S.C., Urbancic, T.I., and Prince, M., Passive Seismic Imaging of Hydraulic Fractures, Ann. Mtg., CSEG, 2002.
- Urbancic, T.I. and Zinno, R.J., Cotton Valley Hydraulic Fracture Imaging Project: Feasibility of determining fracture behavior using microseismic event locations and source parameters, 68th Ann. Mtg. SEG, 964 – 967.

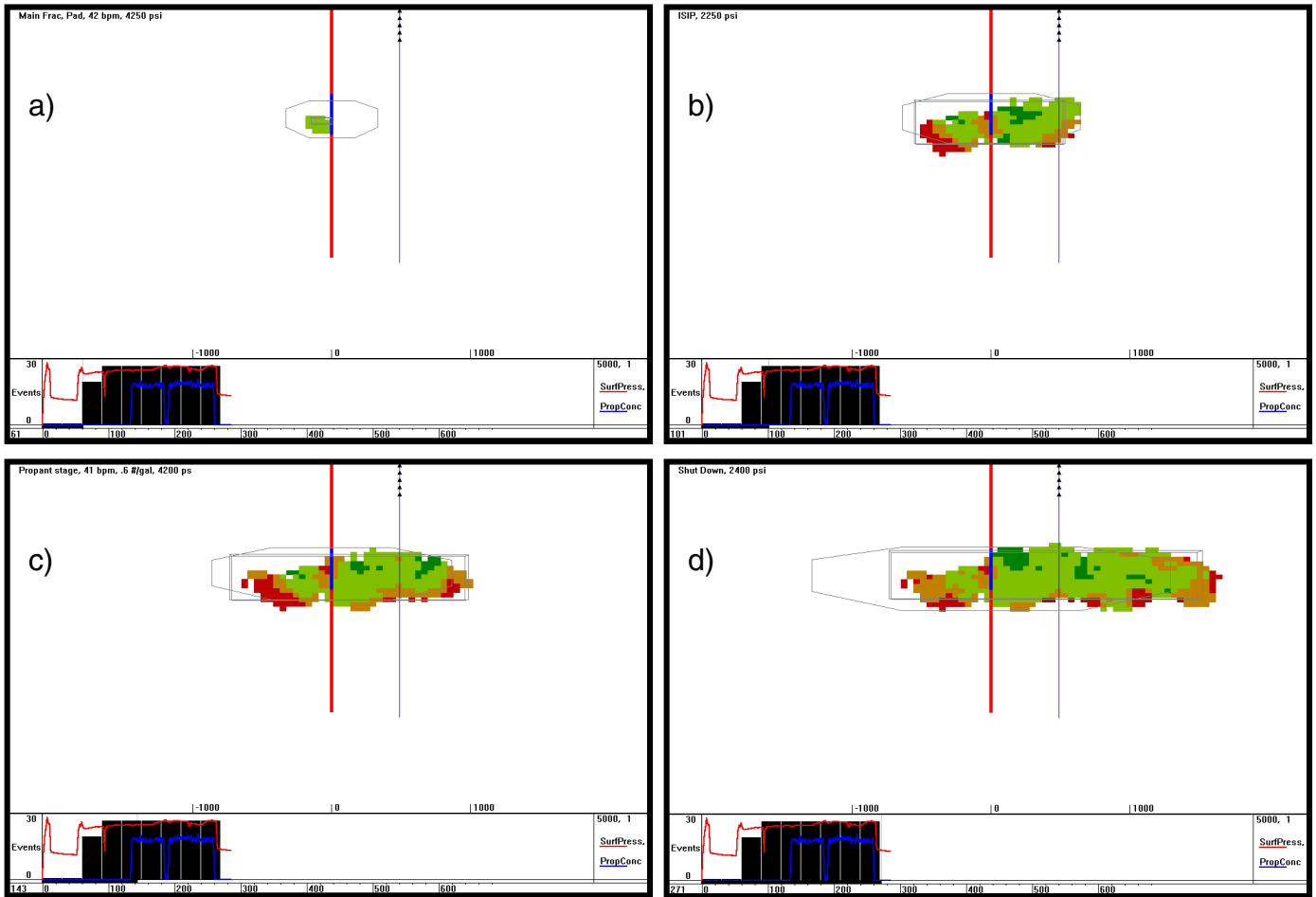


Figure 1. Longitudinal view of depth confined treatment with microseismic events contoured by their apparent stress release values. Low apparent stress values are shown in green whereas larger values are shown in red. The treatment well is shown in red along with the perforation interval in blue. The nearby monitoring well is shown in blue; black triangles represent the geophones in the array.

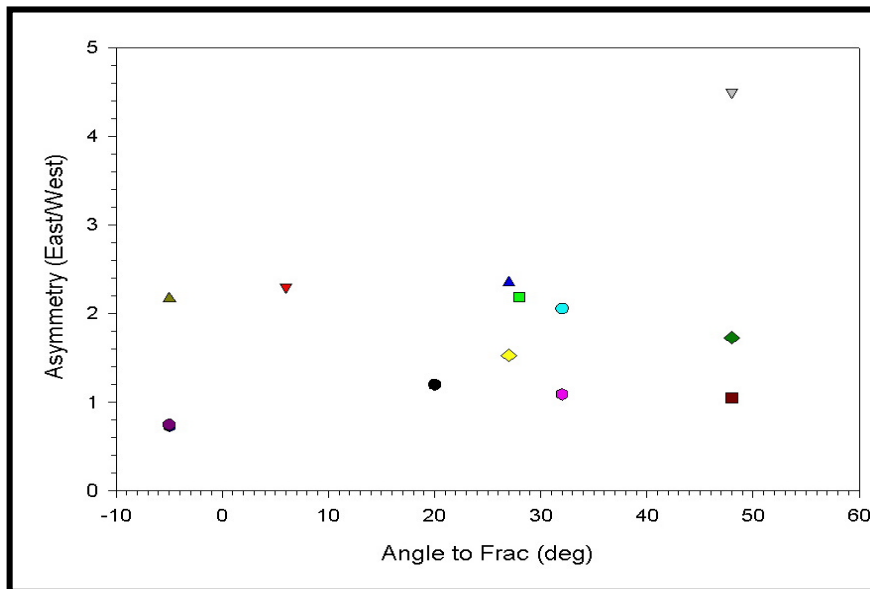


Figure 2. Relative asymmetry for 12 treatments in East Texas. Fracture Symmetry appears to be controlled by the lithology. In this example, treatments were in three lithologic zones corresponding to East wing / West wing symmetries of 1:1, 2:1, > 2:1 (data quality at issue in last case).